crystals

MDPI

Article

A Tetranuclear Ni(II)-Cubane Cluster Molecule Build by Four μ_3-O-Methanolate (MeO) Ligands, Externally Cohesive by Four Unprecedented Bridging μ_2-N7,O6-Acyclovirate (acv-H) Anions

Jeannette Carolina Belmont-Sánchez [1], Duane Choquesillo-Lazarte [2], Ricardo Navarrete-Casas [1], Antonio Frontera [3], Alfonso Castiñeiras [4], Juan Niclós-Gutiérrez [1] and Antonio Matilla-Hernández [1,*]

[1] Department of Inorganic Chemistry, Faculty of Pharmacy, University of Granada, 18071 Granada, Spain
[2] Laboratorio de Estudios Cristalográficos, IACT, CSIC-Universidad de Granada, Avda. de las Palmeras 4, 18100 Armilla, Spain
[3] Departament de Química, Universitat de les Illes Balears, Crta. de Valldemossa km 7.5, 07122 Palma de Mallorca, Spain
[4] Department of Inorganic Chemistry, Faculty of Pharmacy, University of Santiago de Compostela, 15782 Santiago de Compostela, Spain
* Correspondence: amatilla@ugr.es

Abstract: Metal ion interactions with nuclei acids and their constituents represent a multi-faceted and growing research field. This contribution deals with molecular recognition between synthetic purine 17 nucleosides and first-row transition metal complexes, with O- and/or N-amino chelators which are able to 18 engage in intra-molecular N-H···(N or O) and O-H···(N or O) interligand interactions. Crystals of these complexes can also display inter-molecular aromatic π-stacking and/or other non-conventional interactions. In this manuscript, we used 2-(2-aminoethoxy)ethanol (2aee) as a potential N,O(e),O(ol)-chelator for nickel(II). However, unexpectedly, the reaction between $NiCl_2$, acyclovir (acv), and 2aee in methanol afforded parallelepiped apple-green crystals of $[Ni(acv\text{-}H)(MeO)(H_2O)]_4 \cdot 8H_2O$, (**1**) a tetranuclear molecule with an equimolar Ni(II):μ_3-methanolate (1-):μ_2-N7,O6-acyclovirate(1-) (acv-H) ratio. The μ_2-N7,O6-(acv-H) metal-binding pattern (MBP) is unprecedented in terms of both its anionic and bridging roles. The single-crystal X-ray diffraction structure as well as thermogravimetric analysis and the (FT-IR +Vis-UV) spectra of **1** are reported. Theoretical density functional theory (DFT) calculations are used to analyse the antiparallel π-stacking interactions that govern the formation of self-assembled dimers in the solid state.

Keywords: nickel; tetranuclear; molecule; cubane; cluster; methanolate; acyclovirate; crystal structure; thermogravimetry; spectral properties

Citation: Belmont-Sánchez, J.C.; Choquesillo-Lazarte, D.; Navarrete-Casas, R.; Frontera, A.; Castiñeiras, A.; Niclós-Gutiérrez, J.; Matilla-Hernández, A. A Tetranuclear Ni(II)-Cubane Cluster Molecule Build by Four μ_3-O-Methanolate (MeO) Ligands, Externally Cohesive by Four Unprecedented Bridging μ_2-N7,O6-Acyclovirate (acv-H) Anions. *Crystals* **2023**, *13*, 7. https://doi.org/10.3390/cryst13010007

Academic Editor: Lidia Ciccone

Received: 3 December 2022
Revised: 15 December 2022
Accepted: 16 December 2022
Published: 21 December 2022

1. Introduction

The synthetic nucleoside acv (Scheme 1) is a recognised antiviral drug, related to the natural nucleoside guanosine (gua). Since 1982, it has been used to treat infections caused by Herpes zoster and Herpes simplex viruses, as documented in the extensive literature, including increasing crystallographic contributions [1–17].

A search of the Cambridge Structural Database (CSD, version 5.43, release September 2022) for acv-H (without the hydrogen atom on the N1-(lactamic) atom to avoid undesirable restrictions) yields 46 hits, corresponding to 38 different compounds. Three of the relevant structures include anhydrous acv (of two polymorphs, belonging to the monoclinic or orthorhombic space groups, $P2_1/c$ [1] or $P2_12_12_1$ respectively [1,2]), and the other two refer to acv hydrates, namely $3acv \cdot 2H_2O$ or $acv \cdot 0.67H_2O$ [3–5] and $acv \cdot 2H_2O$ [2,4]. Structures of organic adduct cocrystals [1,6,7] and one organic salt [5,6] are also known. However, by far the most numerous of these results correspond to 31 metal complexes, including an 'out-of-sphere' Ru(II) complex (Hacv)mer-$[RuCl_4(NO)(O\text{-dmso})]$ (BOZPAI in CSD) having

the aciclovium(1+) cation, with the additional H^+ proton on its N7 atom [8]. The remaining 30 complexes comprise compounds with acv-metal (M) coordination bonds (the number of compounds reported for each metal ion is indicated in parentheses): Co(II) (1) [9], Ni(II) (1) [10], Cu(II) (18) [11–17], Zn(II) (3) [9–11], Cd(II) (1) [10], Ru(III) (3) [18,19] or Pt(IV) (3) [20–22]. Except for the aforementioned out-of-sphere Ru(II) complex [8], the following coordination modes (or metal binding patterns hereafter MBPs) have been crystallographically proven for the 30 'inner sphere' M-complexes of acv. Specific compounds are listed below with the CSD codes and the reference (an asterisk has been added to compounds where the acv displays two distinct MBPs:

(a) MBP-1: M-N7(acv). This is reported for IPUXIB [15], MENJOE* [22], RALPLAY [16], RUMGAH [17], SIMMOQ [21], UNAPEG [16], ZAYBIK [20].

(b) MBP-2: M-N7(acv) plus intra-molecular interligand H-bonding interaction. The H-bond is of the type N(amine)-H···O6(acv) in BETSOL, BETSUR, BETTAY, BETTEC, BETTUS or BETVAA [11], O(aqua)-H···O6(acv) in CAFVUD [12], HOPBOD, HOPBUJ or HPPCAQ [10], JAJPOA or JAJPUG [9], LUFGIC [19] or O(alcohol)-H···O6(acv) in ARAMOV [18] or LUFGEY [9].

(c) MBP-3: Chelating-N7,O6. This is reported for three Cu(II) complexes where the O6-acv donor occupies a distal coordination site (with Cu-O6 distances ranking between 2.66 to 2.86 Å): BETTIG or BETTOM [11] and HOSQUB [14].

(d) MBP-4: Bridging μ-N7,O(alcohol) only reported for in the Cd(II) compound HOPCAD [10].

(e) MBP-5: Chelating-O(e),O(ol), N7,O6,O(e),O(ol) tetradentate and μ_3-bridging [13]. This has been only reported for the coordination polymer $[\{Cu_2(acv)(\mu_3\text{-}acv)(SO_4)(\mu_2\text{-}SO_4)(H_2O)_4\}\cdot H_2O\cdot MeOH]_n$ (DIDJUY) [13], where neutral acv displays the highest denticity reported for a synthetic nucleoside. This compound was formed with some serendipity in an attempt to explore diethanolamine (DEA) as potential tridentate chelator for Cu(II), thus offering two terminal O(ol)-H groups as candidates for –O-H···O(6)-acv intramolecular interligand interactions.

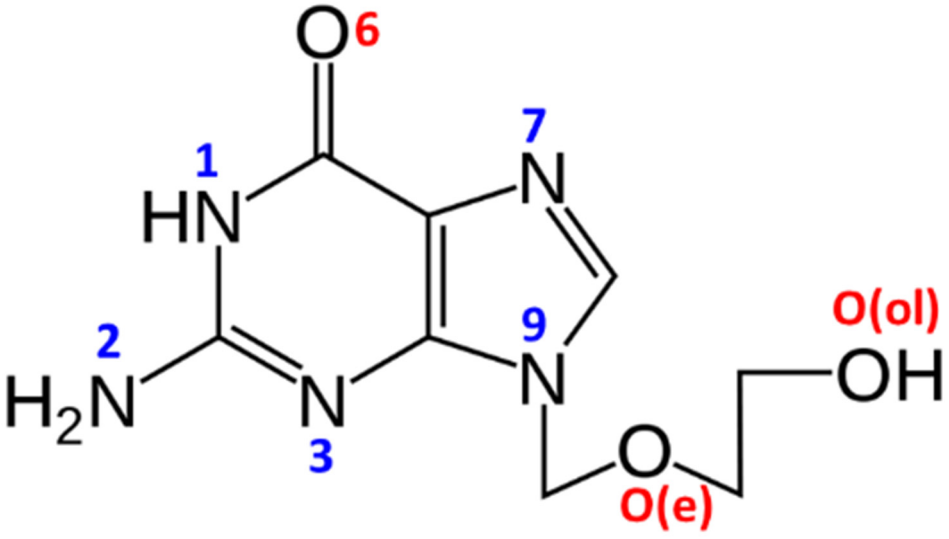

Scheme 1. Acyclovir, with the adopted numbering for N and O atoms.

In summary, it is worth emphasising that: (1) The N7-acv atom is indisputably the preferential acv-donor atom, because it is involved in MBP1 to MBP5. (2) Coligands, such as aqua and small alcohols or appropriate amines (having primary or secondary N-H moieties), strongly favour the cooperation between M-N7 bonds and O- H···O6 or N-H···O6 intramolecular interligand interactions. (3) The eventual coordination of the terminal -O(ol) in the acyclic acv-arm is rarely seen. (4) The use of amino-alcohols (i.e., DEA) as potential chelators can lead, with some serendipity, to some unexpected products,

such as the aforementioned Cu(II)-coordination polymer. Here, we report a new acv derivative obtained by reaction of $NiCl_2$, acv, and 2-(2-aminoethoxy)-ethanol (2aee), with the latter being a potential tridentate chelator. DFT calculations are used to demonstrate the importance of π-stacking interactions in the solid state of this complex, which presents an unprecedented coordination mode of acv.

2. Materials and Methods

2.1. Reagents

Nickel chloride hexahydrate (Aldrich, Darmstadt, Germany), 2-(2-aminoethoxy)-ethanol (2aee, TCI) and acyclovir (3acv·$2H_2O$, Acofarma, Madrid, Spain) were used as received. The used polymorph of acv was tested by its X-ray powder diffraction pattern.

2.2. Synthesis with Relevant Vis-UV and FTIR Spectral Data

Compound **1** was obtained in a two-step process. Firstly, equimolar amounts (0.5 mmol) of $NiCl_2·6H_2O$ and acv·$0.67H_2O$ were reacted in MeOH (50 mL). To the resulting pale green solution was added 0.5 mmol of 2aee in MeOH, as 0.2 mL of a 0.2 M mother solution of 2aee, that was prepared by dilution of pure 2aee (2.5 mL = 50 mmol) with MeOH up to 250 mL. This caused an intensification of the apple-green colour of the reaction mixture. The solution was placed in a crystalliser and then covered with a plastic film and left undisturbed. The very slow evaporation of the solvent produced, after two months, an abundance of single crystals (see supporting information) which were suitable for crystallographic studies in a high yield (~0.15 g, ~80%). Elemental analysis (%): Calc. for $C_{36}H_{76}N_{20}Ni_4O_{28}$: C 29.38, H 5.20, N 19.03, Ni (as NiO) 20.30; Found: C 29.32, H 5.16, N 19.00, Ni 21.30 (as NiO, final residue at 950 °C, in the thermogravimetric analysis (TGA curve). FT-IR spectrum (see Supplementary Material) data [cm^{-1}]: ~3370vbr $\nu_{as}/\nu_{as}(H_2O, NH_2)$, 3212 $\nu_s/\nu_s(H_2O, NH_2)$, 3022w $\nu(C\text{-}H)_{arom}$, 2928, 2904m $\nu_{as}(CH_2)$, 2824w $\nu_{as}(CH_2)$,1672 ν(C=O), ~1634 $\delta(H_2O)$, 1592 $\delta(NH_2)$, 1385sh δ(OH, ol), 1116m $\delta(O(e)C_2)$, 874 $\pi(C\text{-}H)_{arom}$ for only one C-H (usually expected at 900–860). Electronic spectrum (nm): maxima at ~392, 667 (sh = shoulder at ~730) and 1078 nm.

2.3. Crystallography

A bluish green parallelepiped crystal of [Ni(μ_2-N7,O6-acv-H)(MeO)(H_2O)]$_4$·$8H_2O$ (**1**) was mounted on a glass fibre and used for data collection. Crystal data were collected at 100(2) K using a Bruker D8 Venture diffractometer. Graphite monochromated Cu*Kα* radiation (λ = 1.54184 Å) was used throughout. The data were processed with APEX2 [18]. The structure was determined by direct methods, using the SHELXS-2013 program [19] and refined by full-matrix least-squares techniques against F^2 using SHELXL-2013 [19]. The positional and anisotropic atomic displacement parameters were refined for non-hydrogen atoms. Except for two water molecules, the remaining solvent molecules (observed from the difference Fourier maps) could not be identified because of significant disorder and/or partial occupancy; they were SQUEEZE'd out using PLATON [20]. Final refinement included: (a) the split into two positions for O21, C22, C23, and O24 from the (2-hydroxyethoxy)methyl chain (occupancy factors 0.43(1)/0.57(1)), and (b) bond-length restrains DFIX of 1.50(5) Angstrom's for each bond of the C20-O21-C22-C23-O24 chain. The problem of disorder around the (2-hydroxyethoxy)methyl chain gave rise to rather elongated ellipsoids for split C23 and O24 atoms. Hydrogen atoms were located in difference maps and included as fixed contributions riding on attached atoms with isotropic thermal parameters 1.2/1.5 times those of their carrier atoms. The large discrepancy between the *R* and *wR* values was due to the high thermal vibration present in the (2-hydroxyethoxy)methyl chain of aciclovir and crystallisation water molecules. Nevertheless, the final results can be considered satisfactory from a chemical point of view. The criteria of a satisfactory complete analysis were the ratios of root-mean-square (rms) shift to standard deviation being less than 0.001 and no significant features in the final difference maps. The lowest (-0.36 e·$Å^{-3}$) and highest (0.58 e·$Å^{-3}$) peaks in the final

difference Fourier map were located close to crystallisation water molecules at 0.67 and 0.14 Angstroms of C23A and H4A, respectively. Atomic scattering factors were taken from the International Tables for Crystallography [21]. Molecular graphics were elaborated with PLATON [20] and DIAMOND [22]. A summary of the crystal data, details of the experiments, and refinement results are listed in Table 1.

Table 1. Crystal data and structure refinement for [Ni(μ_2-N7,O6-acv-H)(MeO)(H_2O)]$_4$·8H_2O (**1**).

Empirical Formula	**$C_{36}H_{76}N_{20}Ni_4O_{28}$**
Formula weight	1472.00
Crystal system, space group	Cubic, $Fd\bar{3}c$
Unit cell dimensions	a = 48.916(3) Å, α = 90°
	b = 48.916(3) Å, β = 90°
	c = 48.916(3) Å, γ = 90°
Volume	117,045(22) Å^3
Z, Calculated density	48, 1.002 Mg/m^3
Absorption coefficient	1.407 mm^{-1}
F(000)	36,864
Crystal size	0.120 × 0.030 × 0.030 mm
Theta range for data collection	5.115 to 66.848°
Limiting indices	$-57 \leq h \leq 58$, $-57 \leq k \leq 51$, $-57 \leq l \leq 58$
Reflections collected/unique	389,455/4285 [R_{int} = 0.0845]
Completeness to θ = 67.679	96.6%
Absorption correction	None
Refinement method	Full-matrix least-squares on F^2
Data/restraints/parameters	4285/32/237
Goodness-of-fit on F^2	1.161
Final R indices [I > 2σ(I)]	R_1 = 0.0780, wR_2 = 0.2227
R indices (all data)	R_1 = 0.0795, wR_2 = 0.2243
Largest diff. peak and hole	0.578 and –0.356 e.Å^{-3}
CCDC ref. number	2223304

2.4. Other Physical Measurements

Analytical data (CHN) obtained in a Fisons–Carlo Erba EA 1108 elemental microanalyser. The nickel(II) content was cheeked as NiO by the weight of final residue in the thermo-gravimetric analysis (TGA) at 950 °C within <1% of assumed experimental error. The FT-IR spectrum was recorded (KBr pellet) on a Jasco FT-IR 6300 spectrophotometer. The electronic (diffuse reflectance) spectrum was obtained with a Varian-Cary5E spectrophotometer. TGA was carried out (r.t. −950 °C) in airflow (100 mL/min) using a Shimadzu Thermobalance TGA–DTG–50H, while a series of 37 time-spaced FT-IR were spectra recorded with a coupled FT-IR Nicolet Magna 550 spectrometer to identify the evolved gasses.

2.5. Theoretical Methods

The binding energy of the dimeric assembly analysed in this manuscript was computed using the Gaussian-16 program [23], as the energy difference between the dimeric assembly and twice the energy of the monomer. The basis set superposition error (BSSE) was minimised using the approximation proposed by Boys and Bernardi approach [24]. Since we are interested in analysing the interaction as it stands in the solid state, the X-ray coordinated values were used. Consequently, frequency calculations were not carried out, since the geometry was not optimised. For the calculations, the triple-ζ, def2-TZVP [25] basis set was used in combination with the hybrid PBE0 functional [26] and Grimme's D3 dispersion correction [27]. The Molecular Electrostatic Potential (MEP) surface of the monomer was computed using the 0.001 isosurface at the same level of theory. The NCI index [28] and QTAIM [29] were calculated using the AIMAll program [30] at the same level of theory.

3. Results and Discussion

3.1. Molecular and Crystal Structure of the Novel Compound

Compound **1** consists of a tetranuclear Ni(II)-cubane cluster molecule and non-coordinated water molecules, according to the formula $[Ni(acv\text{-}H)(MeO)(H_2O)]_4 \cdot 8H_2O$. In all structural figures, the disorder in the acyclic arm of the acv-H anion, referred to in Section 2.3, is omitted for clarity. Figure 1 shows the asymmetric unit of its crystal. Figure 2 represents tetranuclear Ni(II)-cubane cluster molecule. Table 2 summarises the coordination and other interatomic distances, as well as the trans-Ni-coordination angles. A photograph of the crystals and some additional structural information are reported in the supporting information.

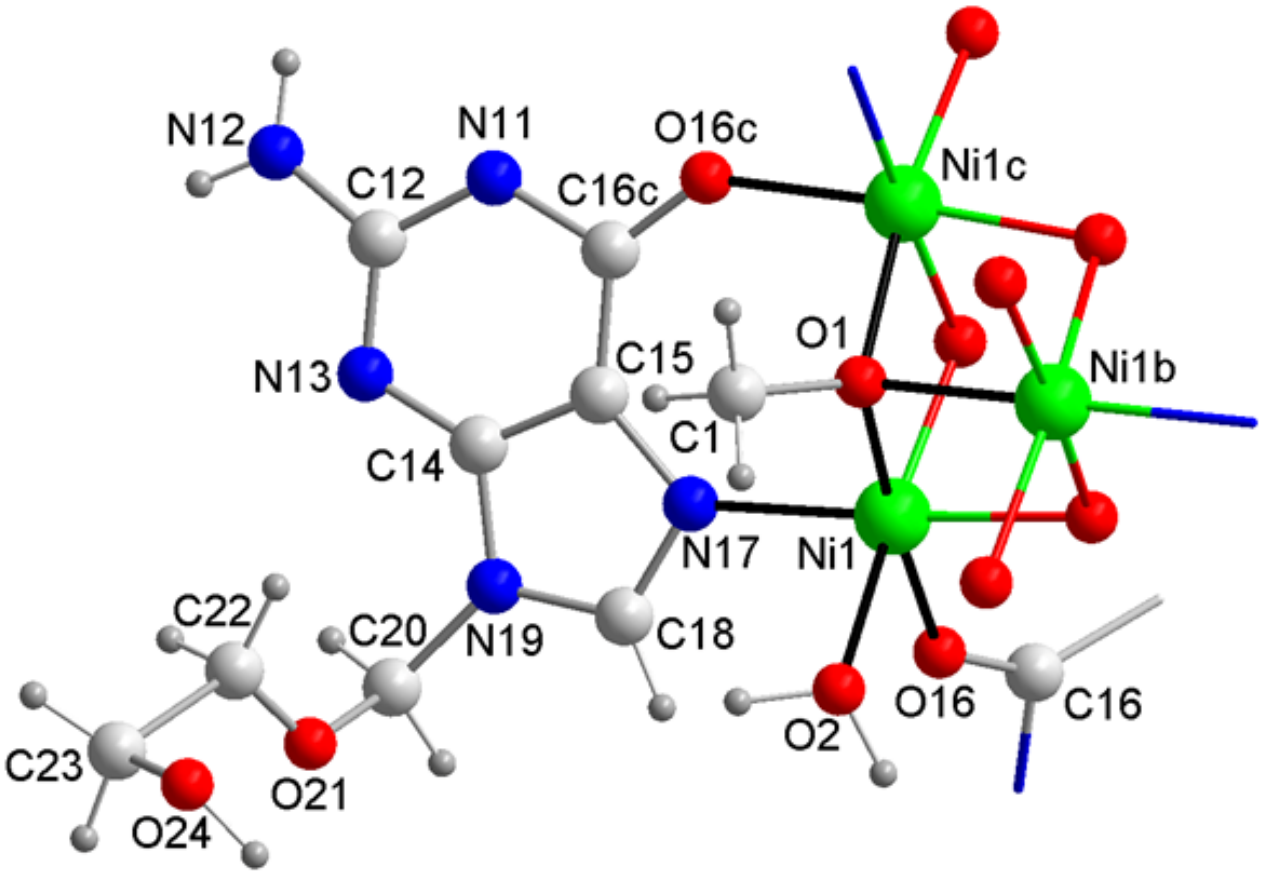

Figure 1. The asymmetric unit in the crystal of **1**, with the numbering scheme for non-hydrogen atoms. Symmetry codes: b = #2 = −x + 1/4,y,−z + 1/4, c = #3 = z,−y + 3/4,−x + 1/4.

The tetranuclear cluster molecule of **1** is defined by two interpenetrated tetrahedral sets of Ni(II) centres and O1-μ_3-methanolate donors, these last atoms being what play the primary role for its construction (Figure 3). Therefore, both the interatomic distances Ni1···Ni1 (3.05 ± 0.01 Å) and O1···O1 (2.70 ± 0.01 Å) are each other reasonably similar. All six faces of this cube have two Ni(II) centres arranged in opposite vertices, which furthermore are peripherally held together by four acyclovirate(1-) anions, displaying the unprecedented and bridging MBP μ-N7,O6(acv-H) (Figure 2). In this case the intermetallic Ni···Ni distance is 3.05 Å (vide supra) whereas the interatomic N7···O6 distance within the acv-H ligand is 3.17 Å.

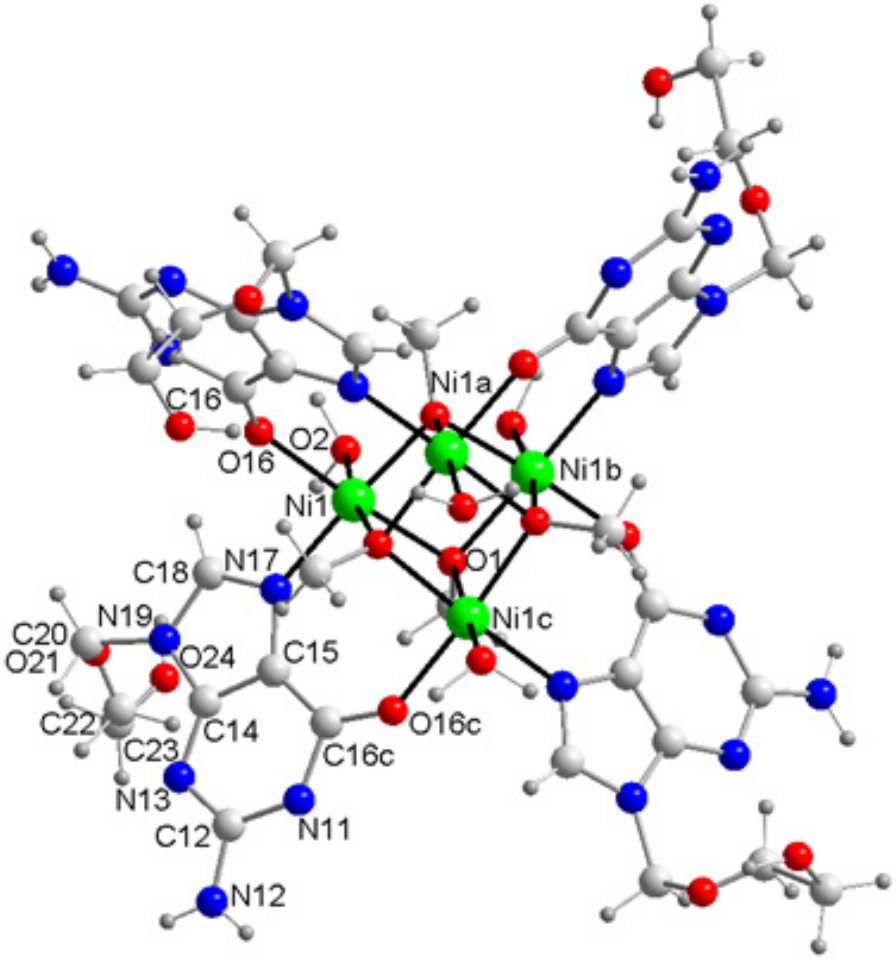

Figure 2. The tetranuclear Ni(II)-cubane cluster molecule of **1**. Symmetry codes: a = # 1 = −z + 1/4, −y + 3/4,x, b = #2 = −x + 1/4,y,−z + 1/4, c = #3 = z,−y + 3/4,−x + 1/4.

Table 2. Coordination bond lengths and other relevant inter-atomic distances (Å) and trans-coordination angles (°) in the crystal of compound **1**, $[Ni(acv\text{-}H)(MeO)]_4 \cdot 8H_2O$. See also Figures 1 and 2 for the numbering of non-H atoms.

Atoms	Distance (Å) or Angle (°)
Ni(1)-O(1)#1	2.041(3)
Ni(1)-O(1)	2.038(2)
Ni(1)-O(1)#2	2.049(2)
Ni(1)-O(16)	2.054(2)
Ni(1)-N(17)	2.069(4)
Ni(1)-O(2)	2.131(3)
Ni(1)-Ni(1)#1	3.0527(10)
Ni(1)-Ni(1)#2	3.0657(11)
Ni(1)-Ni(1)#3	3.0527(10)
O(1)-O(1)#1	2.701(4)
O(1)-O(1)#2	2.694(5)
O(1)-O(1)#3	2.701(4)
O(1)-Ni(1)-(O16)	175.74(10)
O(1)#2-Ni(1)-N(17)	176.76(12)
O(1)#1-Ni(1)-O(2)	171.96(11)

Symmetry codes: # 1 = −z + 1/4,−y + 3/4; x; #2 = −x + 1/4,y,−z + 1/4; #3 = z,−y + 3/4,2x + 1/4.

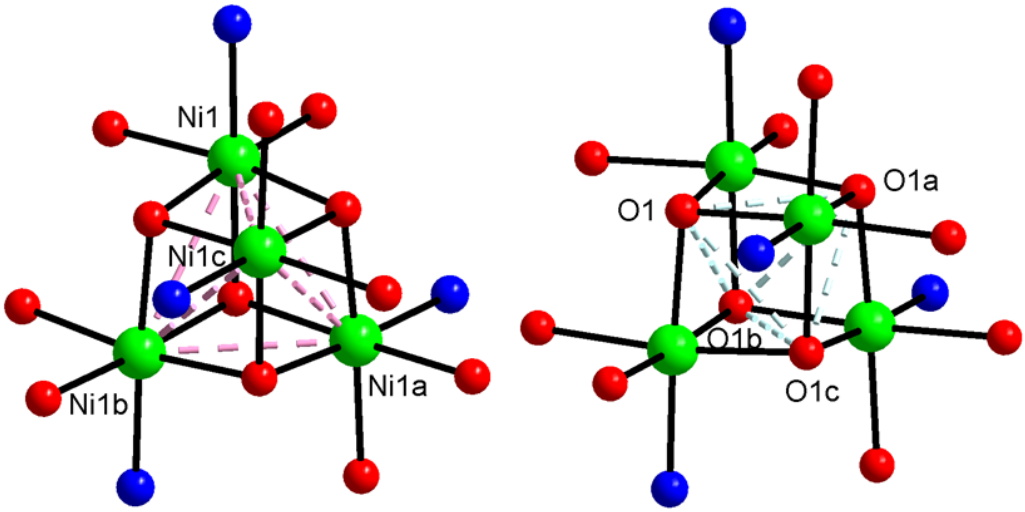

Figure 3. Interpenetrated tetrahedral set of four Ni(II) centers and four O1 donors by four μ_3-O-methanolate ligands, as primary driving force in the building of the tetranuclear core of **1**.

Each μ-N7,O6(acv-H) keeps together two nickel(II) atoms, in such manner that they are arranged on four parallel faces of the cubane cluster. With respect to these, the two remaining faces, upper or lower, contain aqua ligands of respective metallic centres. Thus, the tetranuclear molecule contains an equimolar ratio of its four constituents, Ni(II) centres, μ_3-methanolate, μ-N7,O6-acyclovirate and aqua, in such a manner that each metal centre satisfies its octahedral coordination. Interestingly, the averaged Ni1-O1(methanolate) distance (2.04 Å) corresponds to the shortest bonds, whereas the Ni1-O2(aqua, neutral) bond (2.14(1) Å) is the largest one. Also the anionic nature of the μ-N7,O6(acv-H) ligand (after deprotonating the N1-H lactam of acv) yields Ni-N7 and Ni-O6 bond distances (averaging ~2.06 Å) similar to the Ni-O(methanolate) ligands (see Table 2).

The crystal is built by two types of intermolecular forces. Firstly, by a slipped π-stacking interaction between the pyrimidine rings of two acv-H ligands, connecting each cluster with four neighbours (Figure 4): inter-centroids distance d_{c-c} 3.76 Å, inter-planar distance $d_{\pi-\pi}$ 3.40 Å, dihedral angle 0 or 1.3°, slipping angles β or γ 25.3°. These interactions build supramolecular framework running parallel to the ac crystal plane. At a second level, two H-bonds are involved connecting the before referred frameworks: O(2)-H(2A)···O(4)#4 (2.714(6) Å, 159.8°, #4 = y,z,x) and N(12)-H(12A)···O(4)#5 (2.935(6), 156.4°, #5 = −x,−y + 1/2,−z + 1/2). Both of them have the same water molecule as acceptor. Interestingly the –O(ol) seems to be not involved in this kind of interaction, which may favour the disorder observed in the acyclic arm of acv-H ligands (see experimental Section 2.3).

3.2. Theoretical Study

Initially, the molecular electrostatic potential (MEP) surface of compound **1** was computed to analyse the most electron-rich and -poor parts of the molecule (see Figure 5). The MEP maxima are located at the H-atoms of the coordinated water molecules (+49 kcal/mol), followed by the H-atom of the alcohol (+48 kcal/mol). The MEP values at the H-atoms of the exocyclic amino group are significantly less positive (+30 kcal/mol). The MEP minimum is located at the N1-atom (−46 kcal/mol) and is significantly more negative than that at N3 (−34 kcal/mol).

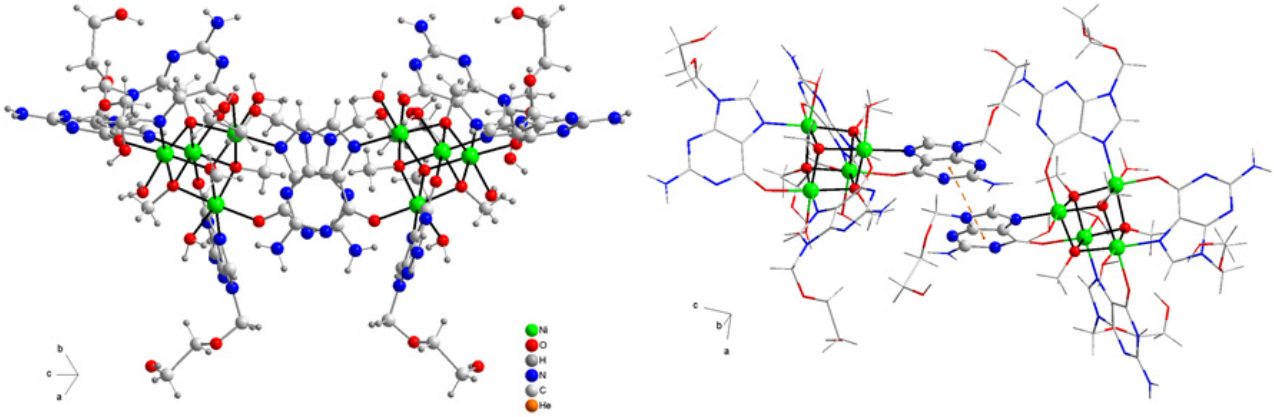

Figure 4. Two images illustrating the π-staking interactions between the six-membered pyrimidine rings of two acv-H ligands from two neighbouring cluster molecules of compound **1**.

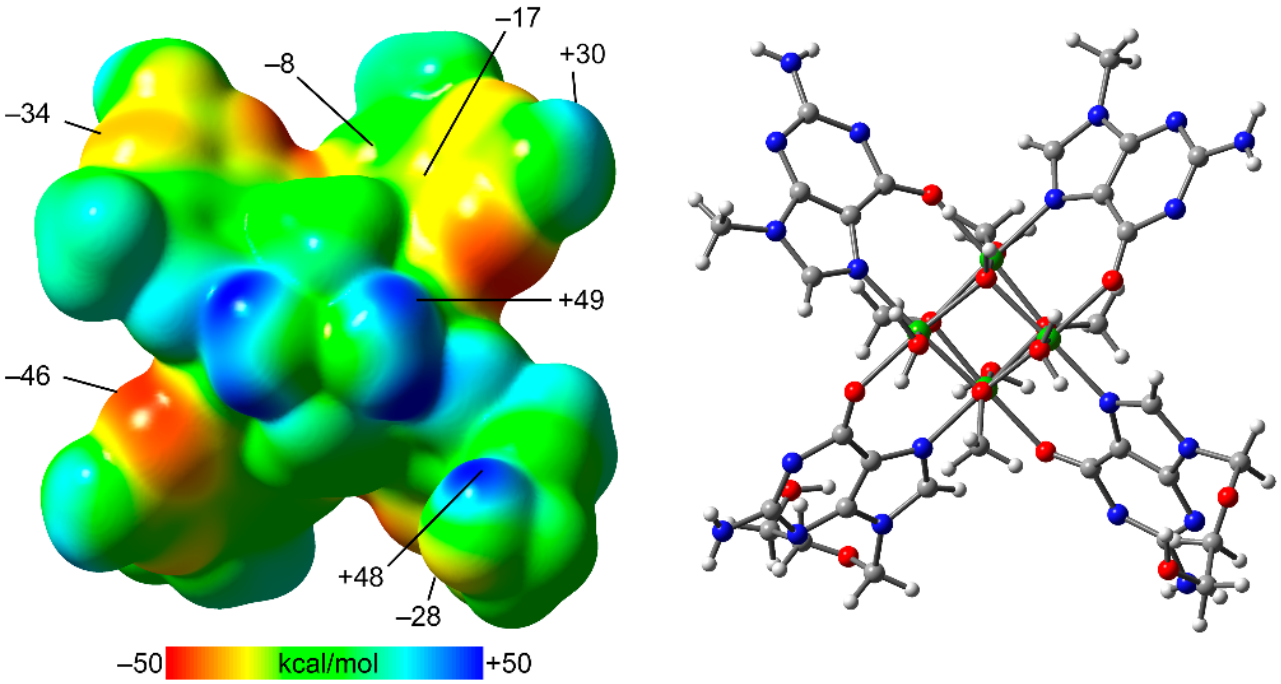

Figure 5. (**Left**) MEP surface of compound **1** at the PBE0-D3/def2-TZVP level of theory. The energies in kcal/mol. (**Right**) Representation of the molecule in the same orientation used to plot the MEP surface.

This MEP surface analysis reveals the existence of potentially strong H-bond donor/acceptor groups in this molecule. However, H-bonds between the acyclovir moieties are not observed in the X-ray structure of **1**, likely due to the presence of the co-crystallised water molecules that form H-bonds with some of these groups, hindering the formation of acv···acv H-bonding assemblies.

The most important force in the solid state of compound **1** is the π-stacking interaction between the coordinated acv ligands, as described above in Figure 4. This has been analysed herein using DFT calculations and the QTAIM and NCIPlot computational tools, since both methods are useful to reveal interactions in real space. It can be observed that the π···π stacking interaction is characterised by six bond critical points (CP, small red spheres in Figure 6) and bond paths (represented as dashed bonds) interconnecting the acv rings. Interestingly, the QTAIM analysis indicated the participation of the exocyclic NH_2 group in the stacking interaction. Moreover, the interaction is further characterised by a large and green reduced density gradient (RDG) isosurface that encompasses the whole space

between the six membered rings and partially the five membered rings. The dimerisation energy is large (−25.4 kcal/mol), confirming the strong nature of theπ-stacking interaction and importance in the packing of **1**. The NCIplot analysis also reveals the existence of attractive interaction between the pendant acyclic arms of acyclovir of one monomer and the π-system of the acv moiety of the adjacent monomer. As shown in the bottom-right part of Figure 6, several green RDG isosurfaces are located between the acyclic arm and the π-system, suggesting the existence of CH···π interactions. Additional van der Waal interactions are also present between both acyclic arms characterised by small and green RDG isosurfaces. Finally, the QTAIM/NCIplot analysis also discloses the existence of weak CH···N bonds involving the H-atoms of the coordinated methoxy groups and N3-atom of acv. Such intricate combination of interactions likely contributes to the formation of the π-stacked assembly and justify the large dimerisation energy.

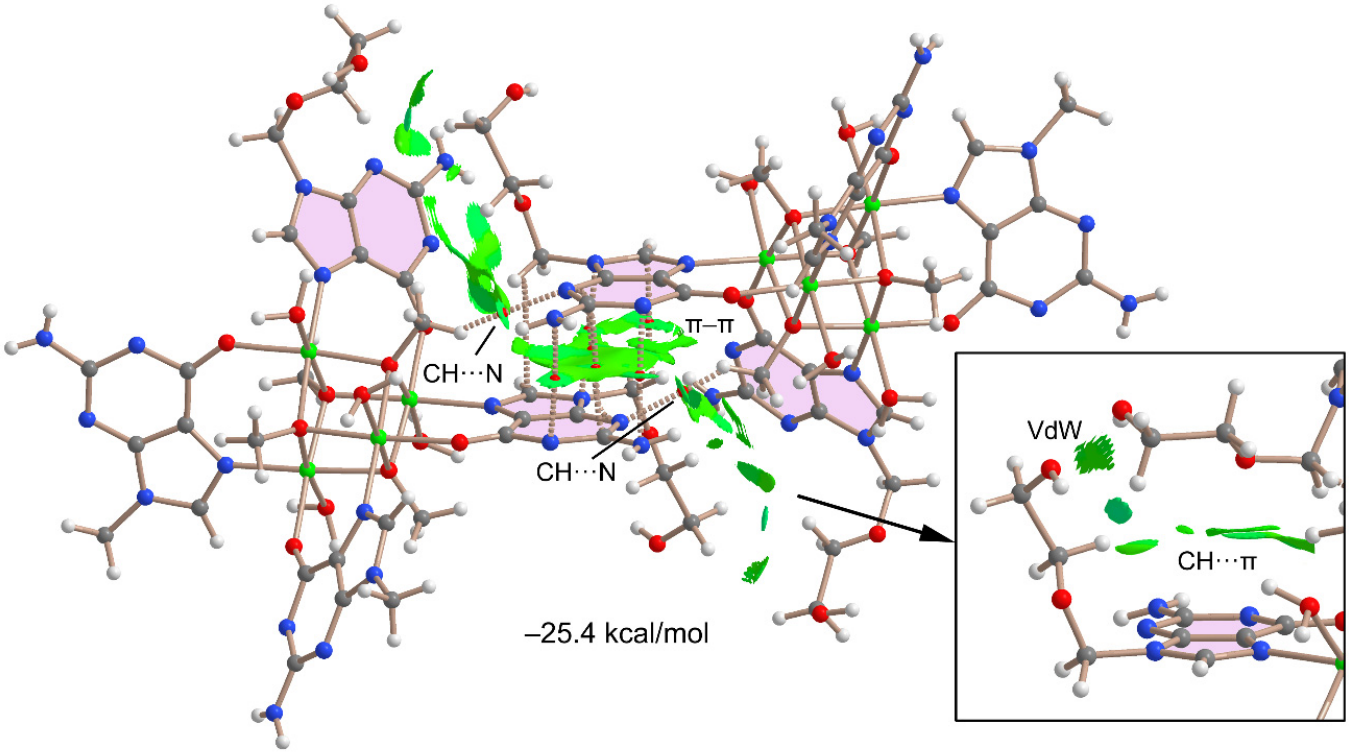

Figure 6. QTAIM analysis (bond CPs in red and bond paths as dashed bonds) and NCI plot analysis [(signλ_2) × ρ scale: ±0.03, ρ cut-off 0.04 a.u.] of the π-stacked assembly of compound **1**. Only intermolecular interactions are represented.

3.3. Spectral Properties and Thermal Stability

The FT-IR spectrum of **1** is provided in the Supplementary Material, with the wavenumbers of most relevant bands. Those reported in Section 2.2 are of relevant diagnostic values and agree with the content of acyclovir and water in **1**. However, from this spectrum, it is unclear that 2aee or methanol(ate) are also present in the novel compound because their IR chromophores are also in acyclovir. It is also rather unclear whether acv is in an anionic form (acv-H). However, from the moment that the molecular and crystalline structure of **1** is known, this spectrum (like any other of a pure sample) is of normal interest (because of its 'fingerprint) in determining that successive samples produced in the synthesis correspond to the same compound.

The electronic spectrum of **1** (Figure 7) is typical of Ni(II) complexes with octahedral coordination polyhedron. It shows bands with maxima at 392, 667, ~730 (shoulder), and 1078 nm. As is well known, the rather symmetrical band with maximum near 1100 cm^{-1} (related to the electronic transition $^3A_{2g} \rightarrow {}^3T_{2g}$) enables a direct estimation of Δ_o (9260 cm^{-1}) for **1**. These bands occur at 400, 660, ~725, and 1175 nm in the spectrum of the $[Ni(H_2O)_6]^{2+}$

ion (Δ_o 8500 cm^{-1}). The hypochromic displacement observed in the spectrum of **1** is mainly due to the anionic nature of its methanolate and acv-H ligands, because only one O-aqua donor of **2** is replaced by an N-heterocyclic one in **1**.

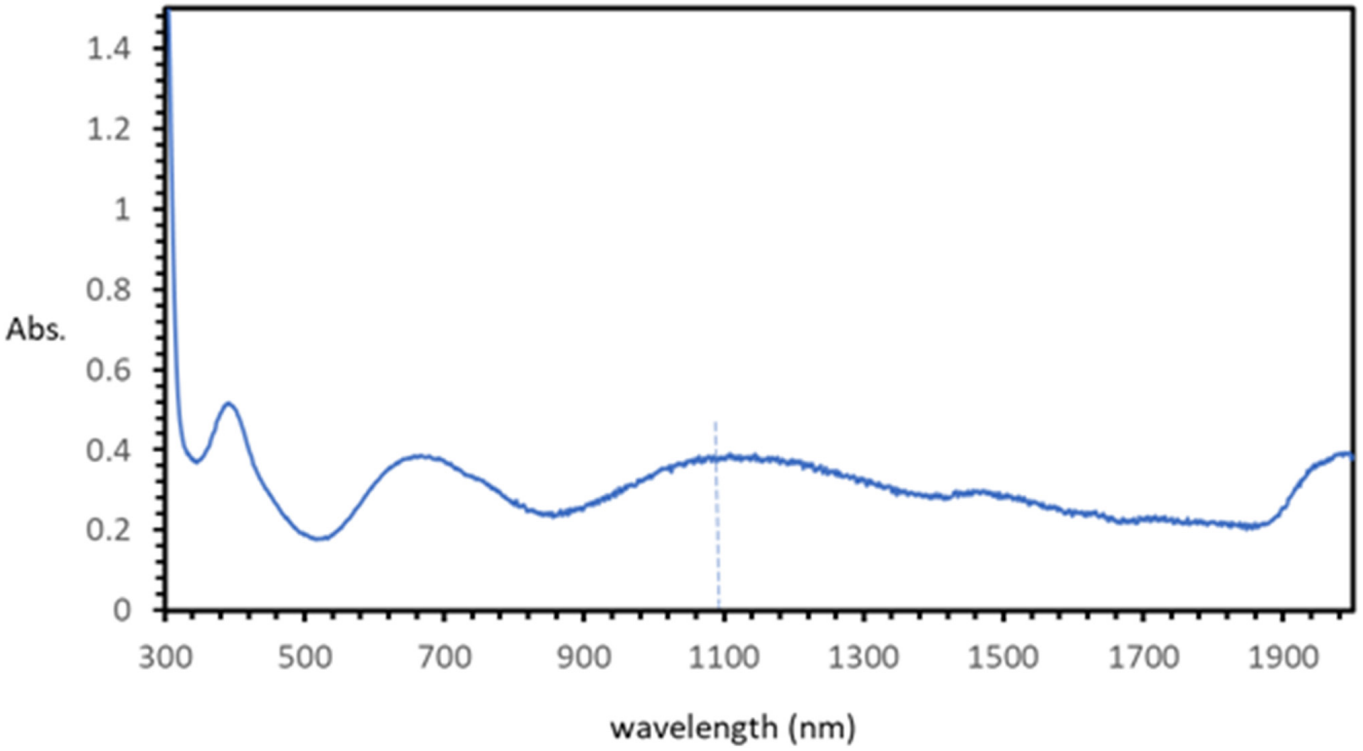

Figure 7. The electronic (diffuse reflectance) spectrum of compound **1**.

The thermogravimetric behaviour of **1** is shown in the TGA plot (Figure 8), where dashed lines are placed looking at the minima in its first derivative in a routine manner to define the successive steps (see the Supplementary Materials for further description).

Some brief comments are required about the water loss (steps 1 and 2) and the final residue yielding NiO (see Table 3). First, non-coordinated water molecules (but not the aqua ligands) were lost during the two first steps. Nevertheless, practical difficulties to accurately locate the end of the second one (probably at ~265 °C) explain the difference between the experimental loss and the calculated one (>1%). In turn, this implies a remarkable thermal stability of the cluster molecule of **1**. Indeed, the surprising production of the volatile and flammable MeOH occurred among the gases evolved during steps 3 and 4. On the other hand, the quantity of residue observed at the end of step 4 (23.913%, at 750 °C) exceeded the calculated value for a residue of nickel oxide (20.300%); however, reasonable agreement (within a 1%) was achieved at the end of step 5 (20.300%, at 950 °C).

3.4. A Critical Look at the Role of 2aee in the Synthesis of Two Closely Related Compounds

The role of the diethanolamine (DEA) in the synthesis of the $[\{Cu_2(acv)(\mu_3\text{-}acv)(SO_4)(\mu_2\text{-}SO_4)(H_2O)_4\}\cdot H_2O\cdot MeOH]_n$ remains unclear [13]. A detailed consideration of its structure reveals that it contains both monodentate acv in MBP-1 and multifunctional acv in MBP-5, whereas DEA is not part of its composition. The role of DEA as a base completely rules this out, since both acv ligands act in a molecular (not anionic) form. However, a search in the CSD database for the chelation of DEA to first-row transition metal ions (1R) affords 31 items (1R = Cr-Zn), including mono- and hetero-nuclear complexes having bidentate- and/or tridentate molecular (DEA) or anionic (DEA-2H) forms. The crystal structures of seven Ni-DEA derivatives are reported, with bidentate N,O-DEA [31–33] or tridentate N,O_2-DEA [34–36]. Regarding this work, attention must be paid to the cationic complex of $[Ni_4(damo)_4(DEA)_2(DEA\text{-}H)_2]\ (ClO_4)_2\cdot 2H_2O$ (damo = diacetylmonoximate(1-) anion)

MABNOW. In this case, the 12-MC-4 type metallacrown has a slightly distorted square planar Ni_4-motif (Ni-Ni' 3.40–3.45 Å, Ni-Ni'-Ni" 89.34–90.90°). In clear contrast, the novel cluster molecule has anionic acv-H, revealing that 2aee acts as a base which is strong enough to deprotonate the N1-H lactam bond of acv.

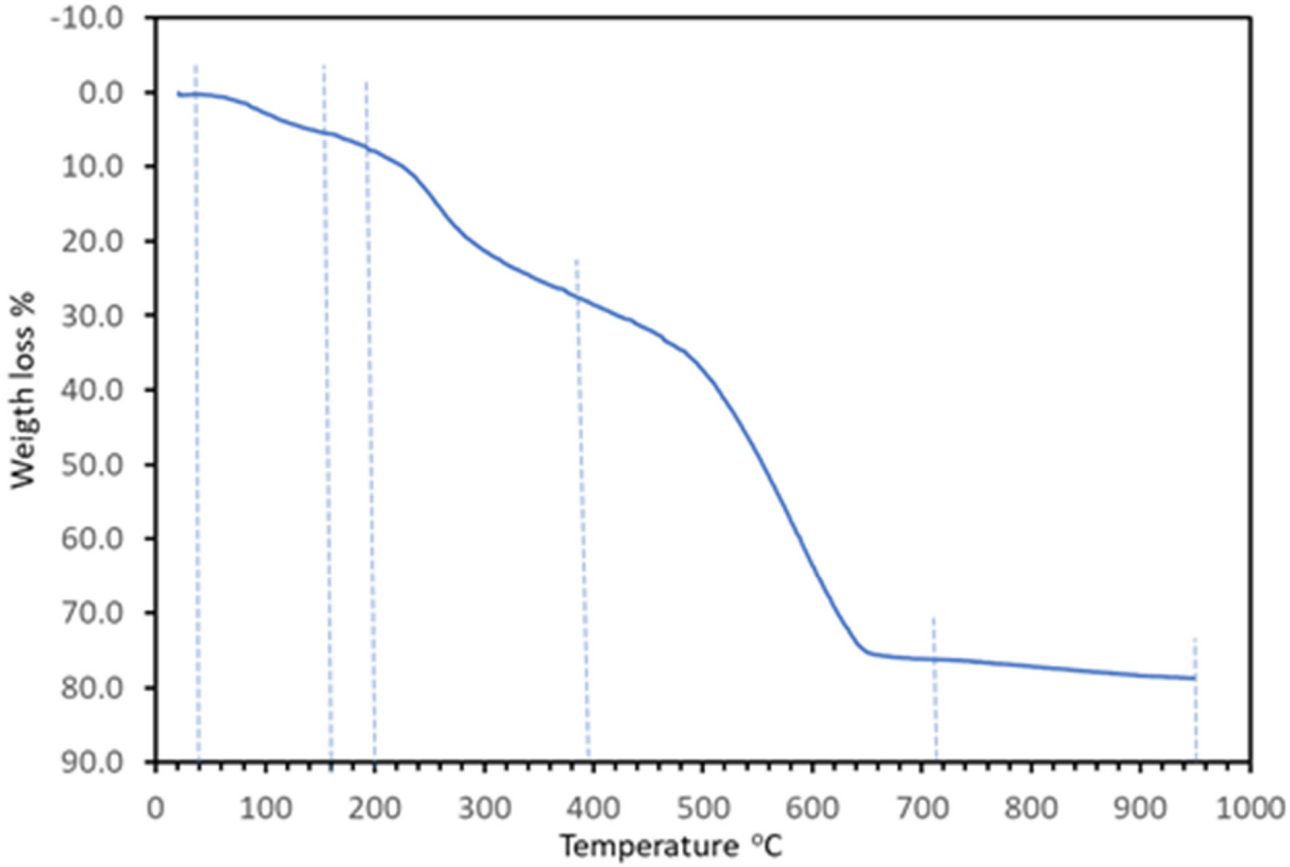

Figure 8. Weight loss versus temperature (r.t. to 950 °C) in the TGA analysis of **1** (sample: 9.382 mg).

Table 3. Summary of results obtained from the thermogravimetric analysis of compound **1**.

Step or R	Temp. (°C)	Time (min)	Weight (%) Exp.	Weight (%) Cal.	Evolved Gases or Residue (R)
1	40–160	3–15	5.351		$4H_2O$, CO_2 (t)
2	160–200	15–18	2.265	-	~4 H_2O, CO_2 (t)
(1 + 2)	(40–200)	(3–18)	(7.616) *	(9.792) *	~8 H_2O, CO_2 (t)
3	200–395	18–38	20.179	-	H_2O, CO_2, CO, MeOH
4	395–715	38–70	48.2.92	-	H_2O, CO_2, CO, MeOH, CH_4 (t), N_2O, NO, NO_2
5	715–950	70–93	2.474	-	H_2O (t), CO_2 (t)
R	950	93	21.303	20.300	4 NiO

* In parenthesis, data of the first plus second steps, (t) = Trace amounts. R = solid residue.

The deprotonating of methanol can be induced by its bridging function between Ni(II) centres, to the point of enabling its μ_3-O role, thereby favouring the construction of the tetranuclear Ni(II)-cubane cluster molecule reported here. This observation finds support in the stoichiometry of the synthesis, which provides the amount of 2aee required to deprotonate the acv. In fact, a higher proportion of 2aee induces the hydrolysis of the metal, generating its precipitation as $Ni(OH)_2 \cdot nH_2O$. Moreover, in contrast to the diversity of coordination modes reported for DEA (molecular or anionic) documented with crystallographic support, a query in the CSD database on 2aee does not yield any result.

Additionally, it is significant that the dissociation of N1-H (lactam) from acv does not lead to the metal-binding of the N1(anionic form); this evidences the potential formation of the Ni-N1(acv-H) bond (a monodentate mode) in favour of the unprecedented bidentate bridging MBP, μ-N7,O6 for acyclovir(ate).

4. Concluding Remarks

Serendipitously, the attempt to obtain a ternary Ni-acyclovir-[2-(2-aminoethoxy)-ethanol] metal complex afforded the novel compound $[Ni(acv\text{-}H)(MeO)(H_2O)]_4 \cdot 8H_2O$, a hydrated form of the tetranuclear Ni(II)-cubane cluster molecule. Its synthesis and crystal structure determination represent the first structural contribution with anionic form of acyclovir and the unprecedented (while bridging) metal binding pattern μ-N7,O6, versus the currently known diversity of coordination modes reported for molecular acv. At the same time, the misguided use 2aee as a potential tridentate chelator for nickel(II) in this work revealed the possibility of its utilisation in future works with the anionic form of acyclovir.

Supplementary Materials: The following supporting information can be downloaded at: https://www.mdpi.com/article/10.3390/cryst13010007/s1, Figure S1: Crystals of compound $[Ni(\mu_2\text{-}N7,O6\text{-}acv\text{-}H)(\mu_3\text{-}MeO)(H_2O)]_4 \cdot 8H_2O$ (**1**).; Structural parameters, TGA curves and IR information.

Author Contributions: Conceptualisation, A.M.-H. and J.N.-G.; methodology, all authors; software, A.M.-H., A.C., A.F. and A.C.; investigation, J.C.B.-S. and R.N.-C.; writing—original draft preparation, all authors, writing—review and editing, all authors; visualisation, A.C., D.C.-L., A.F. and A.M.-H. project administration, A.C., A.F., A.M.-H. and J.N.-G.; funding acquisition, A.C., A.F. and J.N.-G. All authors have read and agreed to the published version of the manuscript.

Funding: This research was funded by MICINN of Spain (project PGC2018-102047-B-I00), MICIU/AEI of Spain (project PID2020-115637GB-I00, FEDER), Project B-FQM-478-UGR20 (FEDER-Universidad de Granada, Spain) and the Research groups FQM-283 and FQM-243 (Junta de Andalucía, Spain).

Data Availability Statement: Not applicable.

Acknowledgments: We thank the Centre de Tecnologies de la Informació (CTI) at the University of the Balearic Islands (UIB) for the use of their computational facilities.

Conflicts of Interest: The authors declare no conflict of interest.

References

1. Tutughamiarso, M.; Wagner, G.; Egert, E. Cocrystals of 5-fluorocytosine. I. Coformers with fixed hydrogen-bonding sites. *Acta Crystallogr. Sect. B* **2012**, *68*, 431–443. [CrossRef] [PubMed]
2. Terada, K.; Kurobe, H.; Ito, M.; Yoshihashi, Y.; Yonemochi, E.; Fujii, K.; Uekusa, H. Polymorphic and pseudomorphic transformation behavior of acyclovir based on thermodynamics and crystallography. *J. Therm. Anal. Cal.* **2013**, *113*, 1261–1267. [CrossRef]
3. Birnbaum, G.I.; Cygler, M.; Kusnierek, J.T.; Shugar, D. Structure and conformation of the potent antiherpes agent 9-(2-hydroxyethoxymethyl)guanine (acycloguanosine). *Biochem. Biophys. Res. Commun.* **1981**, *103*, 968–974. [CrossRef]
4. Birnbaum, G.I.; Cygler, M.; Shugar, D. Conformational features of acyclonucleotides: Structure of acyclovir, an antiherpes agent. *Can. J. Chem.* **1984**, *62*, 2646–2652. [CrossRef]
5. Luker, K.M.; Quiñones, R.; Ramamoorthy, A.; Matzger, A.J. Polymorphs and hydrates of acyclovir. *J. Pharm. Sci.* **2011**, *100*, 949–963. [CrossRef]
6. Yan, Y.; Chen, J.-M.; Lu, T.-B. Simultaneously enhancing the solubility and permeability of acyclovir by crystal engineering approach. *CrystEngComm* **2013**, *15*, 6457–6460. [CrossRef]
7. Wang, L.; Zhao, Y.; Zhang, Z.; Wang, J.; Wang, Q.; Zheng, Z.; Deng, Z.; Zhang, H. Polymorphs of acyclovir-maleic acid salt and their reversible phase transition. *J. Mol. Struct.* **2017**, *1127*, 247–251. [CrossRef]
8. Golobic, A.; Saric, D.; Turel, I.; Serli, B. Crystal structure of ionic compound between antiviral drug acyclovir and complex ruthenate(II). *Acta Chim. Slov.* **2008**, *55*, 973–977.
9. Barceló-Oliver, M.; Terrón, A.; García-Raso, A.; Fiol, J.J.; Molins, E.; Miravitlles, C. Ternary complexes metal [Co(II), Ni(II), Cu(II) and Zn(II)]–ortho-iodohippurate (I-hip)–acyclovir. X-ray characterization of isostructural $[(Co, Ni \text{ or } Zn)(I\text{-}hip)_2(ACV)(H_2O)_3]$ with stacking as a recognition factor. *J. Inorg. Biochem.* **2004**, *98*, 1703–1711. [CrossRef]
10. García-Raso, A.; Fiol, J.J.; Bádenas, F.; Cons, R.; Terrón, A.; Quirós, M. Synthesis and structural characteristics of metal–acyclovir (ACV) complexes: $[Ni(or\ Co)(ACV)_2(H_2O)_4]Cl_2 \cdot 2ACV$, $[Zn(ACV)Cl_2(H_2O)]$, $[Cd(ACV)Cl_2] \cdot H_2O$ and $[\{Hg(ACV)Cl_2\}_x]$. Recognition of acyclovir by Ni–ACV. *J. Chem. Soc. Dalton Trans.* **1999**, 167–174. [CrossRef]

11. Pérez-Toro, I.; Domínguez-Martín, A.; Choquesillo-Lazarte, D.; García-Rubino, M.E.; Gónzalez-Pérez, J.M.; Castiñeiras, A.; Bauzá, A.; Frontera, A.; Niclós-Gutiérrez, J. Copper(II) polyamine chelates as efficient receptors for acyclovir: Syntheses, crystal structures and dft study. *Polyhedron* **2018**, *145*, 218–226. [CrossRef]
12. Vílchez-Rodríguez, E.; Pérez-Toro, I.; Bauzá, A.; Matilla-Hernández, A. Structural and Theoretical Evidence of the Depleted Proton Affinity of the N3-Atom in Acyclovir. *Crystals* **2016**, *6*, 139. [CrossRef]
13. Pérez-Toro, I.; Domínguez-Martín, A.; Choquesillo-Lazarte, D.; González-Pérez, J.M.; Castineiras, A.; Niclós-Gutiérrez, J. Highest reported denticity of a synthetic nucleoside in the unprecedented tetradentate mode of acyclovir. *Cryst. Growth Des.* **2018**, *18*, 4282–4286. [CrossRef]
14. Turel, I.; Anderson, B.; Sletten, E.; White, A.J.P.; Williams, D.J. New studies in the copper(II) acyclovir (acv) system. NMR relaxation studies and the X-ray crystal structure of $[Cu(acv)_2(H_2O)_2](NO_3)_2$. *Polyhedron* **1998**, *17*, 4195–4201. [CrossRef]
15. Brandi-Blanco, M.P.; Choquesillo-Lazarte, D.; Domínguez-Martín, A.; González-Pérez, J.M.; Castiñeiras, A.; Niclós-Gutiérrez, J. Metal ion binding patterns of acyclovir: Molecular recognition between this antiviral agent and copper(II) chelates with iminodiacetate or glycylglycinate. *J. Inorg. Biochem.* **2011**, *105*, 616–623. [CrossRef] [PubMed]
16. González-Pérez, J.M.; Choquesillo-Lazarte, D.; Domínguez-Martín, A.; Vílchez-Rodríguez, E.; Pérez-Toro, I.; Castiñeiras, A.; Arriortua, O.K.; García-Rubiño, M.E.; Matilla-Hernández, A.; Niclós-Gutiérrez, J. Metal binding pattern of acyclovir in ternary copper(II) complexes having an S-thioether or S-disulfide NO_2S-tripodal tetradentate chelator. *Inorg. Chim. Acta* **2016**, *452*, 258–267. [CrossRef]
17. Turel, I.; Bukovec, N.; Goodgame, M.; Williams, D.J. Synthesis and characterization of copper(II) coordination compounds with acyclovir: Crystal structure of triaquabis [9-{(2-hydroxyethoxy)-methyl}guanine] copper(II) nitrate (V) hydrate. *Polyhedron* **1997**, *16*, 1701–1706. [CrossRef]
18. *Bruker APEX2 Software v2010.3-0*; Bruker AXS Inc.: Madison, WI, USA, 2010.
19. Sheldrick, G.M. A Short History of SHELX. *Acta Crystallogr. Sect. A* **2008**, *64*, 112–122. [CrossRef]
20. Spek, A.L. Structure validation in chemical crystallography. *Acta Crystallogr. Sect. D* **2009**, *65*, 148–155. [CrossRef]
21. Wilson, A.J.C. *International Tables for Crystallography*; Kluwer Academic Publishers: Dordrecht, The Netherlands, 1995; Volume C.
22. Brandenburg, K.; Putz, H. *DIAMOND 3.x*; Crystal Impact GbR: Bonn, Germany, 2004. Available online: https://www.crystalimpact.com/diamond (accessed on 20 December 2022).
23. Frisch, M.J.; Trucks, G.W.; Schlegel, H.B.; Scuseria, G.E.; Robb, M.A.; Cheeseman, J.R.; Scalmani, G.; Barone, V.; Petersson, G.A.; Nakatsuji, H.; et al. *Gaussian 16*; Revision B.01; Gaussian, Inc.: Wallingford, CT, USA, 2016.
24. Boys, S.F.; Bernardi, F. The calculation of small molecular interactions by the differences of separate total energies. Some procedures with reduced errors. *J. Mol. Phys.* **1970**, *19*, 553–566. [CrossRef]
25. Weigend, F. Accurate Coulomb-fitting basis sets for H to Rn. *Phys. Chem. Chem. Phys.* **2006**, *8*, 1057–1065. [CrossRef] [PubMed]
26. Adamo, C.; Barone, V. Toward reliable density functional methods without adjustable parameters: The PBE0 model. *J. Chem. Phys.* **1999**, *110*, 6158–6169. [CrossRef]
27. Grimme, S.; Antony, J.; Ehrlich, S.; Krieg, H. A consistent and accurate ab initio parametrization of density functional dispersion correction (DFT-D) for the 94 elements H-Pu. *J. Chem. Phys.* **2010**, *132*, 154104–154119. [CrossRef] [PubMed]
28. Contreras-Garcia, J.; Johnson, E.R.; Keinan, S.; Chaudret, R.; Piquemal, J.P.; Beratan, D.N.; Yang, W. NCIPLOT: A program for plotting non-covalent interaction regions. *J. Chem. Theory Comput.* **2011**, *7*, 625–632. [CrossRef]
29. Bader, R.F.W. Atoms in molecules. *Chem. Rev.* **1991**, *91*, 893–928. [CrossRef]
30. Keith, T.A. *TK Gristmill Software, version 13.05.06*; AIMAll: Overland Park, KS, USA, 2013.
31. Ibrahimov, A.; Ashurov, J.; Ibrahimov, A.; Zakirov, B.; (Uzbekistan Academy of Sciences, Tashkent, Uzbekistan). CCDC 1444749: Experimental Crystal Structure Determination. Personal communication, 2017. [CrossRef]
32. Audhya, A.; Maity, M.; Bhattacharya, K.; Clerac, R.; Chaudhury, R. Tri- and Tetranuclear Nickel(II) Inverse Metallacrown Complexes Involving Oximato Oxygen Linkers: Role of the Guest Anion (Oxo versus Alkoxo) in Controlling the Size of the Ring Topology. *Inorg. Chem.* **2010**, *49*, 9026–9035. [CrossRef]
33. Yilmaz, V.T.; Karadag, A.; Thone, C.; Herbst-Irmer, R. Trans-bis(diethanolamine)bis(isothiocyanato)nickel(II). *Acta Crystallogr. Sect. C* **2000**, *56*, 948–949. [CrossRef]
34. Nesterov, D.S.; Makhankova, V.G.; Vassilyeva, O.Y.; Kokozay, V.N.; Kovbasyuk, L.A.; Skelton, B.W.; Jezierska, J. Assembling novel heterotrimetallic Cu/Co/Ni and Cu/Co/Cd cores supported by diethanolamine ligand in one-pot reactions of zerovalent copper with metal salts. *Inorg. Chem.* **2004**, *43*, 7868–7876. [CrossRef]
35. Yamaguchi, R.; Yamasaki, M.; Sakiyama, H. Structure of bis(2,2′-iminodiethanol-N,O,O′)-nickel(II) hydrogen-bonded to an organoboron coordination complex. *X-ray Struct. Anal. Online* **2015**, *31*, 19–20. [CrossRef]
36. Yamaguchi, R.; Yamasaki, M.; Sakiyama, H. Dimeric Structure of a Nickel(II) Complex with 2,2′-Iminodiethanol Composed by the Hydrogen-Bonding Network. *X-ray Struct. Anal. Online* **2014**, *30*, 53–54. [CrossRef]